International Journal of Thermophysics, Vol. 25, No. 1, January 2004 (© 2004)

Reference Microgravity Measurements of Liquid Phase Solute Diffusivities in Tin- and Aluminum-Based Alloys

J. P. Garandet,[1,2] G. Mathiak,[1,3] V. Botton,[4,5] P. Lehmann,[4] and A. Griesche[6,7]

Received November 9, 2002

This paper presents results of the measurement of solute diffusivities in the Al–Ni and Sn–Bi–In systems. These experiments were conducted in microgravity and may therefore be assigned as reference values. A dedicated facility, which can be used for processing of four identical samples in parallel, was developed for the experiments under consideration. In addition, a rather thorough analysis of possible error sources in shear cell type experiments is carried out. Comparison with work carried out using magnetic fields to control convective flows, and with previous indirect measurements results, is also provided. A coherent picture emerges from the overall agreement between various measurements, and the data from the current work can thus be considered as reference benchmarks for future experiments. Another conclusion of the present study is that the shear cell technique is well suited for the measurement of solute diffusivities.

KEY WORDS: Al–Ni system; composition measurement uncertainty; convection; error analysis; liquid-phase solute diffusion coefficients; low gravity; Sn–In–Bi system.

[1] Commissariat à l'Énergie Atomique, DRT/DTEN/SMP/LESA, CEA-Grenoble, 17 rue des Martyrs, F-38054 Grenoble Cedex 9, France.
[2] To whom correspondence should be addressed. E-mail: garandet@chartreuse.cea.fr
[3] Visiting Scientist from German Aerospace Center, DLR-RS, Linder Hoehe, D-51170 Cologne, Germany.
[4] EPM-Madylam, ENSHMG, BP 95, F-38402 St. Martin d'Hères Cedex, France.
[5] Present address: LMFA, INSA-Lyon, Bâtiment Joseph Jacquard, 20 avenue Albert Einstein, F-69621 Villeurbanne Cedex, France.
[6] Institute for Material Sciences and Technologies, TU Berlin, Hardenbergstr. 36, D-10623 Berlin, Germany.
[7] Present address: Hahn-Meitner-Institute (HMI) Berlin, Glienicker Str. 100, D-14109 Berlin, Germany.

0195-928X/04/0100-0249/0 © 2004 Plenum Publishing Corporation

1. INTRODUCTION

Numerical codes aiming at process control are now routinely used in the manufacturing metallurgical or crystal growth industries. However, the availability of sufficiently accurate data in terms of liquid-phase solute diffusion coefficients is a mandatory prerequisite for the simulations to provide meaningful results. The required accuracy is not easy to define *a priori*, since it depends on the level of refinement of the numerical model, but a value in the 10 to 20% range is probably acceptable considering the remaining limitations in terms of computer power and of the models themselves. Diffusivity data can also be used for the validation of condensed-matter physics theories, e.g., regarding the temperature or composition-related variations of a diffusion coefficient. However, for the latter application, the required accuracy to discriminate between competing models is much lower, say in the 1 to 2% range.

A variety of techniques has been developed to perform solute diffusion coefficient measurements. Optical methods have great potential in transparent systems [1], but they can not be applied to the metallic or semiconductor alloys. The utilization of radioactive tracer diagnostics in opaque materials seems to be very promising [2]. A number of results have been obtained with measurement techniques based on the quantification of the mass flux under more or less controlled fluid flows, see, e.g., Refs. 3–5. Additional methods consist of deducing a diffusion coefficient from solute segregation profiles in solidification experiments, either from initial solid state transients [6] or quenched liquids [7].

A limitation of these indirect techniques [3–7] is that they all rely on often complex models to derive the diffusion coefficient, and that the validity of the underlying theoretical basis is often questionable, especially if one considers the extreme variety of fluid-flow phenomena. In this sense, the most direct measurement technique is the one using the simplest of models, namely Fick's law [8, 9]. Experiments thus aim at the realization of a one-dimensional composition profile that can be *in situ* [8] or *a posteriori* [9] analyzed. As a matter of fact, the shear cell method was shown to be well adapted to measurements of diffusion coefficients [9–11]. However, even in such a simplified configuration, natural convection, hardly avoidable due to high temperature operation, can also lead to additional solute transport and thus to an overestimation of the derived value.

Convective contamination of diffusivity measurements has been modeled by several groups, including ours [12–14] in a manner that can be traced back to the original work of Taylor [15]. In earlier work, magnetic fields were successfully used to control [14] or strongly damp [16] fluid flow in electrically conducting liquids. An *a priori* obvious way to get rid

of convective effects is to perform the experiments in the microgravity environment of space orbiting platforms. A number of interesting results have thus been reported [17, 18]. In general, low gravity diffusivity values are significantly below their terrestrial counterparts. However, important variations from one experiment to another have been evidenced. They are tentatively attributed to the unavoidable acceleration fluctuations, and to the fact that the fluid flow problem is quite formidable, meaning that one should be very cautious with *a priori* estimates of the convective effects. Various modelling efforts were recently proposed, with the objective of solving the coupled hydrodynamic and solute transport equations [19–24], but some questions still remain.

In any case, the convection phenomena are so complex, both on earth and in microgravity, that there is clearly a need for clean benchmark experiments to assess the various perturbing effects, as well as to check whether the accuracy required to validate condensed-matter physics theories is attainable. However, these goals imply that the benchmark experiments need to be carefully analyzed in terms of error sources to allow a definite conclusion to be drawn.

Our objective in this paper is to present reference results of diffusivity measurements carried out in microgravity within the Agat facility aboard the Foton 12 Russian capsule flight. Our approach is based on a thorough analysis of errors encountered in diffusion coefficient measurements. The experiments reported in the present paper were conducted as part of a larger program, which included the Technical University of Berlin and the University of Karlsruhe with the support of the European (ESA), German (DLR), and French (CNES) space agencies.

The systems studied in the present work were tin- and aluminum-based dilute alloys. Diffusion couples consisting of the pure element (Sn or Al) were matched to half capillaries of respective nominal weight percent compositions Sn–In 0.95–Bi 2.5 and Al–Ni 3.25. The objective of the Sn–In–Bi experiment was to allow comparison with the results of the EPM-Madylam research program on convection control with magnetic fields and with data from a quenched solidification profile measurement [25]. As for the Al–Ni experiment, the system had been featured in previous space experiments [26].

In Section 2, sample preparation, experimental protocol, and the post-flight analysis of the microgravity data are described. The influence of various process related error sources is quantified in Section 3. Section 4 describes the procedure followed to analyze the composition profiles, with a special emphasis on the effect of the accuracy of the concentration measurements. Finally, we discuss in Section 5 the overall assessment of the results, to draw a conclusion on the diffusion coefficient values and the

associated error bars. Comparison with published data, when available, is also provided. We conclude with some brief considerations on possible improvement on the attainable accuracy.

2. EXPERIMENTAL PROCEDURE

Figure 1 shows an idealized view of the diffusion process in shear cell facilities; two rods of homogeneous solid materials are heated past the melting point up to the working temperature and are set in contact to begin the diffusion phase. After a preset time, the liquid vein is separated into independent units that will be cooled separately back to room temperature to yield the final composition profile. Such a procedure avoids solidification-related solute segregation upon cooling and limits the duration of the diffusion phase by the initial and final shear events. For the shear cell thus used, the solution to the transport equation takes the form of an error function, provided that the diffusion coefficient D is the same all along the cell and that the samples are long enough to avoid end effects. An error function least-squares fit of the experimental composition profile thus allows a measurement of D.

The cells used in our microgravity experiment were based on a design from the TU Berlin [9]. They allowed us to process in parallel four identical capillaries having a diameter $\phi = 1.5$ mm and consisting of twenty segments of thickness $h = 3$ mm. The starting materials for the Sn–In–Bi

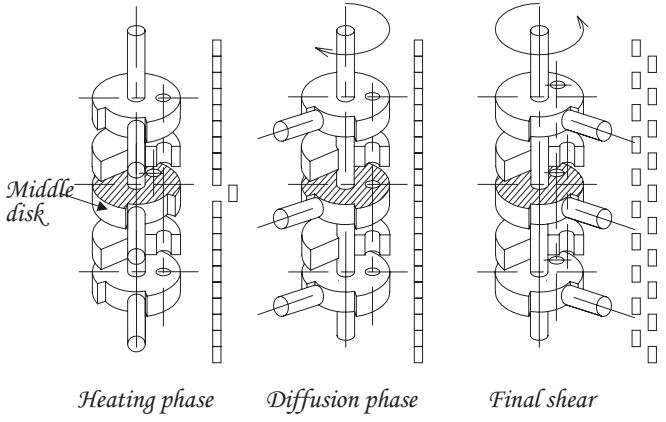

Fig. 1. Principle of diffusivity measurement using the shear cell technique, showing capillary configuration with isolated middle disk during the heating phase, rotation of the middle disk at the beginning of the diffusion phase, and rotation of every other disk at the beginning of the cooling phase.

samples were synthesized in the Grenoble laboratory from 6N sources. Both the aluminum and aluminum-nickel samples were provided by the industrial manufacturer Pechiney, with a reported impurity content less than 300 ppm.

The initial contact is initiated by the rotation of a middle disk (see Fig. 1) to minimize shear-induced convection and associated transport, as demonstrated in parabolic-flight model experiments [27]. On the other hand, the final shear at the end of the diffusion stage is implemented by the rotation of every second disk. The average concentration in each fragment was determined by atomic absorption spectroscopy, and the raw experimental output is thus a discrete 20 steps concentration profile. The design of the cells, especially the aspect ratio $h/\phi = 2$ and the applied shear rate v ($v \approx 100\ \mu\text{m}\cdot\text{s}^{-1}$) comply with rules of thumb resulting from numerical simulations carried out at the NASA Lewis Research Center [28] to identify strategies aiming at mitigating deleterious shearing effects. Still on convection problems, a similar result regarding the influence of the shear rate was observed in Ref. 29. For more information on the shear-cell design and operation, the interested reader is referred to our previous work on the topic [9, 30].

The pre-flight average composition of each capillary was checked to be within $\pm 2\%$ of the nominal value. On the other hand, within a given sample, a concentration scatter of up to $\pm 5\%$ could sometimes be observed. Such a fairly high dispersion is due to a insufficient quenching rate in the elaboration device. Concerning the aluminum cell, the post-flight composition profiles measured on the four capillaries have a close resemblance, as can be seen in Fig. 2. The analysis procedure will be presented in Section 4; however, a preliminary analysis [30] yielded diffusivity values of $\pm 10\%$ between the capillaries, i.e., 3.5 to $3.9 \times 10^{-9}\ \text{m}^2\cdot\text{s}^{-1}$. The observed scatter appeared fairly high and motivated the error analysis carried out in the next sections.

It has first to be stated that a major problem was observed in the tin cell; due to a malfunctioning of the volume control mechanism [30], diffusion barriers were created within 3 of the 4 capillaries, leading to very steep asymmetric composition profiles. These experiments were discarded, but the control volume system fortunately worked well in the fourth capillary, and both the Bi and In composition profiles (see Fig. 3) could be fitted analytically in our preliminary analysis [32]. The values obtained are $D_{\text{In}} = 2.8 \times 10^{-9}\ \text{m}^2\cdot\text{s}^{-1}$ for indium and $D_{\text{Bi}} = 2.3 \times 10^{-9}\ \text{m}^2\cdot\text{s}^{-1}$ for bismuth. However, we first have to discuss the error bar problem before a meaningful comparison with existing literature data can be provided.

Except for the detailed analysis of the influence of the composition measurement accuracy, which will be the subject of Section 4, we shall not

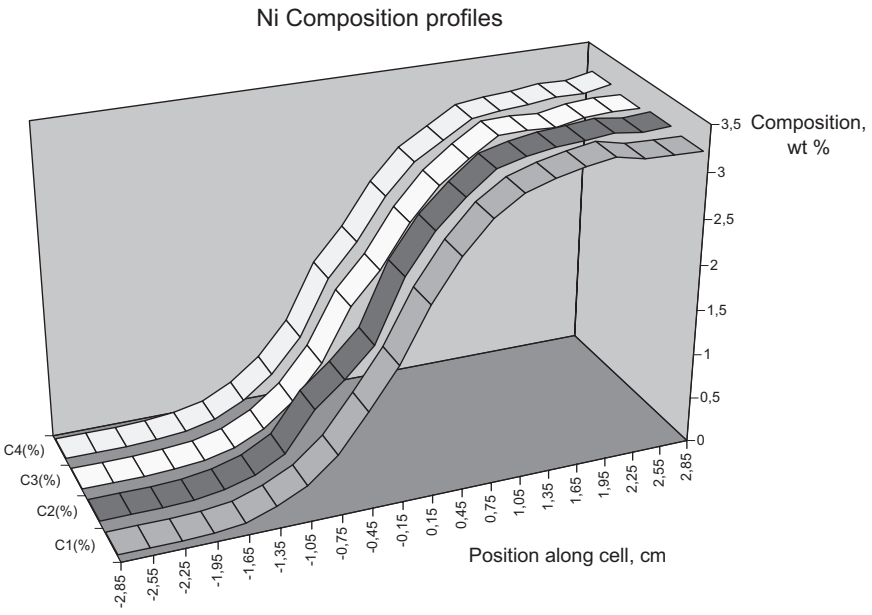

Fig. 2. Nickel composition profiles in the four capillaries of the aluminum cell.

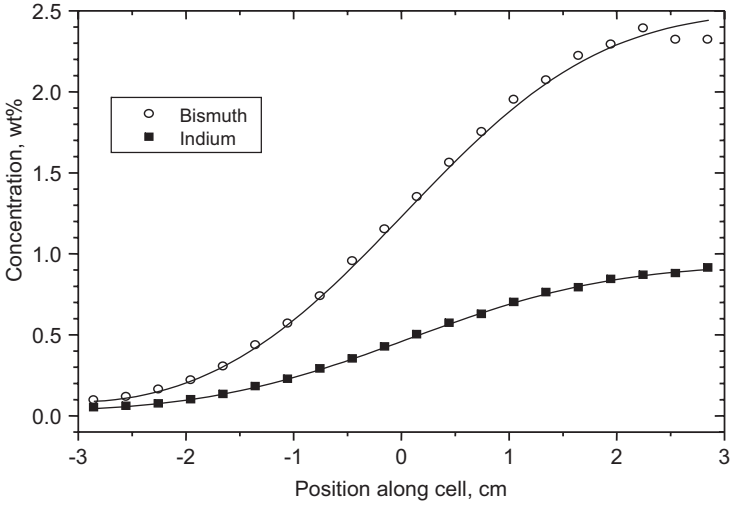

Fig. 3. In and Bi composition profiles in the single useful capillary of the tin cell. Theoretical fits from Fick's equation are shown along with the experimental data.

attempt to define accurately what we mean by error bars in terms of confidence intervals. The Δ signs appearing in the following should be taken as a quantitative assessment of our belief that it is very unlikely to find the exact values outside a $\pm\Delta$ interval. A distinction can be made between process related error sources and uncertainties coming from the composition profile analysis procedure once the experiment is completed. The latter will be the subject of a detailed study in Section 4. At this point, let us first consider process related error sources.

3. EXPERIMENTAL PROCESS ERROR SOURCES

Our purpose in this section is to identify some process related error sources that contribute to the overall measurement accuracy. Whenever possible, quantitative estimates will be given.

3.1. Assessment of Experimental Temperature

The first thing to be mentioned is that the thermal mass of the graphite structure of the experimental device is very large with respect to that of the samples themselves. Considering the fact that the heating zone was larger than the capillary length and the good thermal conductivity of graphite, the temperature field within the cells can be considered relatively homogeneous. For the tin cell, the three thermocouples located within the graphite structure indicated temperature differences of less than 2 K. However, significantly larger differences, of the order of 6 K, were observed within the aluminum cell, which could be partly due to larger heat fluxes towards the cold sinks at the higher working temperature. Another factor to be considered is that the thermocouples were not calibrated prior to the space experiment, meaning that there is an uncertainty of ± 3 K on the measured values. Our choice for the global temperature uncertainty for the tin cell experiments is taken as ± 4 K. Following a similar line, we would have ascribed a ± 6 K uncertainty for the aluminum cell, but we encountered a problem with the temperature regulation, as the control thermocouple started malfunctioning between $t = 10000$ and 12000 s, a possible cause being corrosion.

In any case, this led to a sudden increase of the control thermocouple temperature TC2 from its nominal value of 750°C, as can be seen in Fig. 4. Seeing that, the regulation system imposed a sharp decrease of the power input within the cell, and as a consequence, the actual cell temperature stabilized at a value somewhat below 700°C. Fortunately, a meaningful

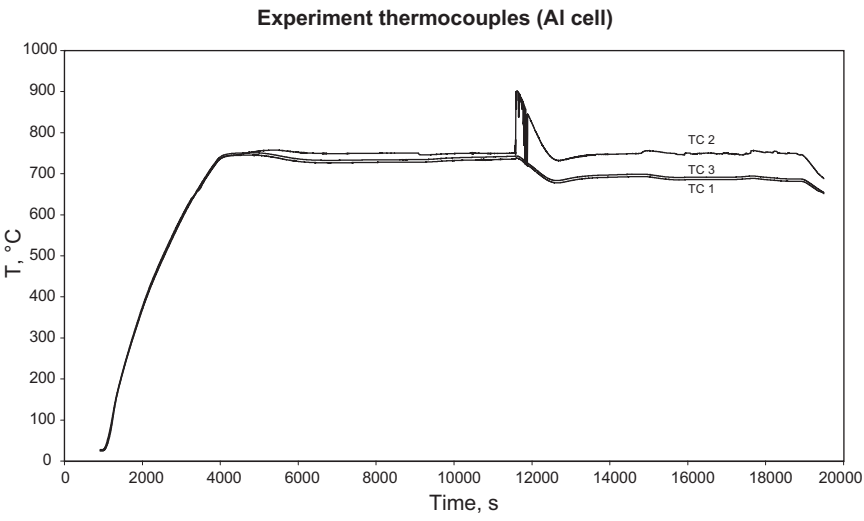

Fig. 4. Time/temperature profile for the aluminum cell experiment.

assignment of the equivalent working temperature can be done based on a change of the time variable in the one-dimensional Fick equation [31]:

$$\partial C/\partial t = D(T(t))\,\partial^2 C/\partial X^2. \tag{1}$$

It is considered in the following that the diffusion coefficient depends on time through its temperature variation $D(T(t))$. If we now set

$$\zeta = \int_0^t D(T(t'))\,dt', \tag{2}$$

it follows quite easily that Eq. (1) can be written as

$$\partial C/\partial \zeta = \partial^2 C/\partial X^2. \tag{3}$$

Let us now assume a diffusion coefficient dependence with the absolute temperature of the form,

$$D(T) = D_0(T/T_0)^n. \tag{4}$$

An important thing to mention is that the temperature dependence featured in Eq. (4) is not arbitrary, as such laws were predicted on the basis of molecular dynamics simulations, with values of n in the range of 1.7 and 2.3.

The next step is to derive ζ by substituting Eq. (4) in Eq. (2), and to select T_0 such that

$$\int_0^t T^n(t')\,dt' = T_0^n t. \tag{5}$$

Then $\zeta = D_0 t$, meaning that Eq. (3) reduces to Eq. (1) with a constant diffusion coefficient D_0. The relevant measurement temperature can be estimated from the signals delivered by the measurement thermocouples TC1 and TC3, which had nominal performance throughout the experiment. The slight difference between the values of TC1 and TC3 observed in Fig. 4 can be explained by the fact that, as stated earlier, the thermocouples were not calibrated, or there were possible residual gradients within the cell. Setting $n = 2$, we find that T_0 equals 968.7 K.

This result depends, of course, on the functional dependence of Eq. (4), but the sensitivity to the exponent n is very small even for unexpectedly large variations with respect to the standard $n = 2$ case. We get, for example, $T_0 = 968.5$ K for $n = 1$ and 968.9 K for $n = 3$. To remain on the safe side, it was decided to set $T_0 = 969$ K and to ascribe a ± 1 K potential error to the procedure for the derivation of T_0. Adding the ± 6 K due to possible residual temperature gradients and uncalibrated thermocouples, the global uncertainty on the aluminum cell is thus ± 7 K. The consequence in terms of the diffusion coefficient itself can be estimated from the relation $\Delta D = (\partial D/\partial t)\,\Delta T$. Using again Eq. (4), we get

$$\Delta D/D_0 = n(\Delta T/T_0). \tag{6}$$

Setting $n = 2$ in the above equation, we obtain $\Delta D/D_0 = 1.4 \times 10^{-2}$. The linear dependence with n is such that a significantly larger uncertainty can be predicted at larger values of n. However, even for $n = 3$, $\Delta D/D_0 = 2 \times 10^{-2}$. To remain on the safe side, our choice was to ascribe this value of 2×10^{-2} to $\Delta D/D_0$.

For the sake of completeness, the same procedure was applied to the mean of the three temperature profiles of the tin cell. As the resulting mean is very smooth, no variations were detected, $T_0 = 573.6$ K for $n = 1, 2, 3$. The error induced by the temperature averaging procedure was neglected, and we decided to set $T_0 = 574$ K, ascribing a ± 4 K value to the global uncertainty associated with possible residual temperature gradients and uncalibrated thermocouples. Using once more Eq. (6) with $n = 2$, we found a value of $\Delta D/D_0 = 1.4 \times 10^{-2}$. To account for the incertitude on the exponent of the power law in Eq. (4), we again ascribed a value of 2×10^{-2} to $\Delta D/D_0$ based on the worst case situation of $n = 3$.

3.2. Duration of Diffusion Phase

We considered so far that the duration of the diffusion period was perfectly characterized with well defined initial and final shear events. In practice, the shearing is done at a rate of $1.5° \cdot s^{-1}$ by a continuous current motor. Completion of the prescribed rotation was assumed when the driving current reaches a threshold value. Taking into account the geometry of the shear cell and the shearing rate of the driving mechanism, the time span corresponding to the situation where the two capillaries are partially in contact could, in principle, be accurately derived for both the initial and final shearing events, and used as a measure of the incertitude on diffusion phase duration. The recorded motor current signals showed that the shearing took place nominally for the tin cell, and we decided to ascribe a $\Delta t = 15$ s uncertainty on each shearing event for the tin cell, which is probably quite overestimated.

Since what is measured is essentially the ratio of a characteristic squared length (here the spread of the initial composition step) λ^2 and the diffusion period duration t, $D \sim \lambda^2/t$, an uncertainty Δt on the experiment duration t_E induces an uncertainty on D such that $\Delta D/D = \Delta t/t_E$. Considering the very long duration of the diffusion period in the tin cell experiment ($t_E = 41076$ s), the relative uncertainty is negligibly small $\Delta t/t_E = 6.6 \times 10^{-4}$.

As for the aluminum cell, we had the problem that the threshold value could not be reached during the 2 minutes security time span for the final shear. *A posteriori* analysis of the cells showed that the shearing did take place, but we are not in a position to estimate when. To remain on the safe side, we thus decided to set $\Delta t = 120$ s, which taken in association with a much shorter diffusion phase duration $t_E = 8124$ s, amounts to a significant relative uncertainty $\Delta t/t_E = 1.5 \times 10^{-2}$.

3.3. Natural Convection Transport

Another process-related error source to be considered is the transport due to convective motions associated with the existence of a residual gravity level in the space experiment. The effect of natural convection in diffusion coefficient measurements has been the topic of many research studies [12–14, 19–24]. The residual gravity in earth orbiting platforms such as Foton is in the 10^{-6} to $10^{-3} g_0$ range depending on frequency, g_0 being the gravity level on earth, but its influence can not *a priori* be neglected. First, a distinction must be made between the low and high ends of the frequency domain, the transition being located around D/ϕ^2, where ϕ is the capillary diameter. In dimensional terms, D/ϕ^2 is of the order of

10^{-3} Hz. However, the models can not be easily applied since no experimental data coming from the gravity sensors were made available for the Foton 12 flight users. We thus had to use data recorded from a similar kind of flight (Foton 11 mission [32]) to assess the additional convective contribution.

In the low frequency end of the spectrum, we decided to set $g = 10^{-5} g_0$, and used the procedure developed in Ref. 12 to estimate that the relative variations of the apparent diffusion coefficient should be very small, say in the 10^{-3} range. As for the high end of the frequency spectrum, in the so-called *g*-jitters domain, the procedure was described in some detail in a recent paper [24], and applied there to the configuration of our Foton experiment, with the conclusion that the induced error was probably very small, again at most in the 10^{-3} range. Overall, we decided to ascribe an experimental uncertainty of $\Delta D/D = 10^{-2}$ to the convection-related error source. This choice may appear somewhat arbitrary, and this 10^{-2} value is probably overestimated, but we need to account for the approximate nature of the theoretical models, and to the fact that some experimental results [18] remain unexplained to this day.

3.4. Graphite Expansion

As mentioned earlier, D can be expressed as the ratio of the square of the spread of the initial composition step to the duration of the experiment, $D \sim \lambda^2/t$. We can thus, in principle, account for the difference in profile spread between room and working temperature coming from the thermal expansion of graphite. Using a thermal expansion coefficient of graphite $\alpha = 7.3 \times 10^{-6}\ \mathrm{K}^{-1}$ along with the formula $\Delta D/D = 2\,\Delta\lambda/\lambda$, we find that the induced uncertainty on D is negligibly small, even in the aluminum cell.

3.5. Shear Convection Induced Problems

The list of potential error sources includes additional mass transport induced by shear convection, mainly due to the initial shear when the concentration step is maximal. The contribution of this effect to the overall mass transport was studied qualitatively in numerous theoretical and experimental investigations and was taken into account in the cell design and the experimental procedure. Quantitatively this effect was measured in short-term diffusion runs in laboratory [9] and parabolic-flight experiments [33]. The system used for these experiments was In–Sn for which convection-free diffusion coefficients $D_{\text{intrinsic}}$ are available [34] measured with the long capillary technique.

Assuming that the measured penetration depth λ is a sum of independent, statistical (quasi-diffusive) transport contributions, a shear-induced additional correction time t_{corr} can be determined, with the consequence that the penetration depth should be modified according to $\lambda\sqrt{(D_{intrinsic}(t_E + t_{corr}))}$. The conclusion is that in the present cases this effect can be neglected for the Sn-based experiment and is very small for the Al-based experiments: $t_{corr}/t_E \approx 0.1\%$.

In the aluminum experiment, another effect related to the initial shearing is the cracking of the covering oxide layer onto the Al-melt surface. The resulting oxide pieces may act as diffusion barriers perturbing the transport process. As this mechanical cracking may differ from one capillary to another, such a mechanism could be invoked to explain the scattering of the D-values for the four independent capillaries. Even though it is possible, in principle, to estimate the effect of various sizes of diffusion barriers on the measured, apparent diffusivity, it should be mentioned that it is not possible, in practice, to specify a relevant input distribution of these barriers. We are unfortunately not in a position to ascribe an error bar to this barrier effect, but an uncertainty in the % range can not be ruled out.

4. CONCENTRATION DATA ANALYSIS PROCEDURE

4.1. Error Function Fit

The post-flight individual samples (20 for each capillary) were analyzed by means of atomic absorption spectroscopy. The raw output of an experiment thus consists of a discrete $N = 20$ steps composition that can be fitted with an error function to extract the diffusion coefficient. The analysis was carried out in parallel at TU Berlin, Madylam, and CEA-Grenoble, and it should be mentioned that one of the results of the present experiment was a uniformization of the analysis procedures used in the various groups. Briefly speaking, the optimization is based on the minimization of the χ^2 defined as

$$\chi^2 = \sum_1^N (C_i^{exp} - C_i^{th})^2/\sigma_i^2 \tag{7}$$

where C_i^{exp} and C_i^{th}, respectively, represent the experimentally measured and theoretically derived compositions, σ_i standing for an estimate of the variance of C_i^{exp}. Two limiting cases for the determination of σ_i can be dealt with, namely (i) absolute uncertainty, when σ_i is independent of C_i^{exp} and (ii) relative uncertainty, when σ_i is proportional to C_i^{exp}. In practice,

a single measurement technique can result in both absolute and relative uncertainties in a given composition profile: the relative accuracy given by the Cermep Institute in Grenoble on their concentration measurements is $\pm 50\%$ at the detection limit $C_i^{\exp} = 0.02$ wt%, $\pm 20\%$ for $C_i^{\exp} = 0.1$ wt%, $\pm 5\%$ for $C_i^{\exp} = 0.5$ wt%, and $\pm 2\%$ for $C_i^{\exp} > 1$ wt%. These values should be understood as given with a high confidence interval, corresponding to at least twice the standard deviation.

In view of the above data, we decided to set $\sigma_i = 0.01$ wt% (absolute uncertainty) for $0 < C_i^{\exp} < 1$ wt%, and $\sigma_i = 0.01 C_i^{\exp}$ (relative uncertainty) for $C_i^{\exp} > 1$ wt%. The fit parameters appearing in C_i^{th}, along with the diffusion coefficient D, are the initial composition within the half capillary C_0 (the starting composition in the other half capillary being zero) and a possible shift x_0 between the geometrical center of the capillary and the location of the initial concentration step [35], such a shift being the result of the volume compensation mechanism. However, other sources of additional transport could also be responsible for the observed shift. This issue, along with further insights on the chi-square fit procedure, is discussed in detail in Ref. 36.

It should be mentioned that units of mass fractions were always used, even though molar or volume fractions are expected to be preferable from a thermodynamic standpoint. However, in dilute alloys, linear relations exist between the various fractions. It was checked in our alloys that the diffusivity results are independent of the choice of units. In addition, the abscissa corresponding to a given composition measurement was taken at the center of the corresponding disk. Effects related to the curvature of the composition profile over a distance of one disk thickness were found to be clearly negligible [10, 37].

In the aluminum cell, the diffusion period was short enough so that no modification of the initial end concentrations was observed, which is a necessary condition for a fit using a single error function [31]. The values obtained in the four capillaries are $D_1 = 3.4 \times 10^{-9}$ m$^2 \cdot$s^{-1}, $D_2 = 4.1 \times 10^{-9}$ m$^2 \cdot$s^{-1}, $D_3 = 3.6 \times 10^{-9}$ m$^2 \cdot$s^{-1}, and $D_4 = 3.5 \times 10^{-9}$ m$^2 \cdot$s^{-1}. The slight but nevertheless significant differences with earlier data [30] are due to the uniformization of the analysis procedures between the various teams involved in the Foton mission.

In the tin cell experiment, a couple of communication failures between the Agat computer and the Foton control unit led to a re-initialization of the computer clock, and thus to a duration of the diffusion period significantly larger than expected, namely 41000 s instead of 22000 s. With such an extended duration, the finite size of the capillaries becomes a factor, and the end compositions within the cell were seen to be slightly modified with respect to their initial values.

In that case, the solution to the diffusion equation with no flux boundary conditions at the ends of the sample takes the form of an infinite series of error functions. A very good approximation for the derivation of the C_i^{th} inputs can be obtained from a truncation of the series to the sum of the first 100 terms, the contribution of the rest having no effect on the final results. The values obtained are $D_{\text{In}} = 3 \times 10^{-9}\ \text{m}^2 \cdot \text{s}^{-1}$ for indium and $D_{\text{Bi}} = 2.4 \times 10^{-9}\ \text{m}^2 \cdot \text{s}^{-1}$ for bismuth, in very close agreement with what had been published as preliminary results [30].

One of the problems raised during the procedure pertains to the homogeneity of the capillaries prior to the diffusion phase. Indeed, as mentioned earlier, pre-flight variations of $\pm 5\%$, due to an insufficient quenching rate in the feed elaboration device, were identified from the AAS analysis. A positive factor is that these variations can be expected to be smoothed out during the high temperature hold prior to the diffusion phase, as well by the diffusion process itself over the duration of the experiment.

Nevertheless, a pre-existing curvature in the capillary composition profile could modify the slope of the $C(X)$ curve even at the end of the experiment. We are unfortunately not in the position to unambiguously assess the uncertainty induced by such concentration variations; all that can be said at this point is that no obvious pre-existing curvature could be identified on the measured composition profiles.

The analysis presented so far assumed Fick's law with a concentration independent diffusion coefficient. This assumption can be checked by means of the Boltzmann–Matano procedure [31], with a change of variables $\xi = X/\sqrt{t}$, that allows expressing the variation of D with distance (and thus with concentration) along the cell as

$$D(C) = (1/2)(dC/d\xi)^{-1} \int_0^C \xi \, dC. \tag{8}$$

In practice, considerable uncertainties are associated with the estimation of the composition gradient around the sample ends where $dC/d\xi$ is very small. This is illustrated in the analysis of the Bi profile in the tin cell shown in Fig. 5, where it is seen that meaningful data can only be obtained in the center of the capillary. In all cases, the Boltzmann–Matano data, though somewhat scattered, indicated the presence of a constant plateau value in the zone that matters most for the determination of the diffusion coefficient.

We did, thus, assume the error function fits of the composition profiles to be justified, even though a $D(C)$ dependence can not be excluded, and it should be recognized that we are not here again in a position to unambiguously ascribe an associated error bar to the measurement coming from

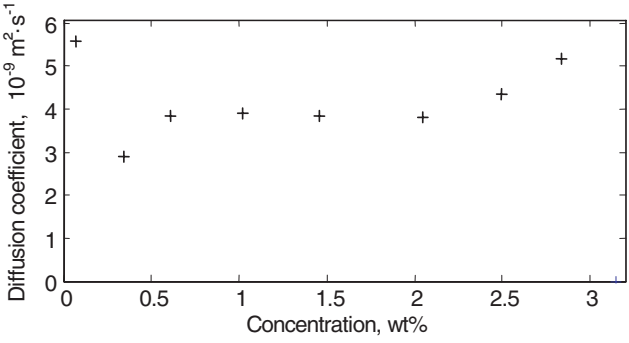

Fig. 5. Boltzmann–Matano analysis for the Ni composition profile in capillary #1 of the Al–Ni cell.

the choice of the physical model. A further hypothesis is that we also assumed that the tin-based alloy was sufficiently dilute for the diffusion of In and Bi to proceed independently of each other, but a small correlation effect can not be excluded.

4.2. Effect of Composition Measurement Uncertainty

The last step in our study is to ascribe a scientifically based error bar to the effect of composition measurements uncertainty. To do so, we relied on Monte-Carlo type simulations, the procedure being as follows:

(i) A theoretical profile is first constructed with C_i^{th} values derived according to Fick's law using the measured diffusion coefficient D_{mes}.

(ii) A Gaussian analysis noise, with variances σ_i, defined as in Section 4.1, is superimposed on the C_i^{th} values, yielding an "experimental" C_i^{exp} profile.

(iii) The obtained "experimental" profile is submitted to the χ^2 minimization procedure to estimate the apparent diffusion coefficient D_{app}.

(iv) Steps (ii) and (iii) are repeated a large number of times (typically 1000) to obtain statistically meaningful information on the distribution of D_{app}.

A typical output of the procedure is shown in Fig. 6, where it can be seen that the D_{app} distribution is indeed Gaussian, with a mean value corresponding to the prescribed diffusion coefficient D_{mes}. The variance σ of this distribution can thus be taken as an estimate of the error coming from the

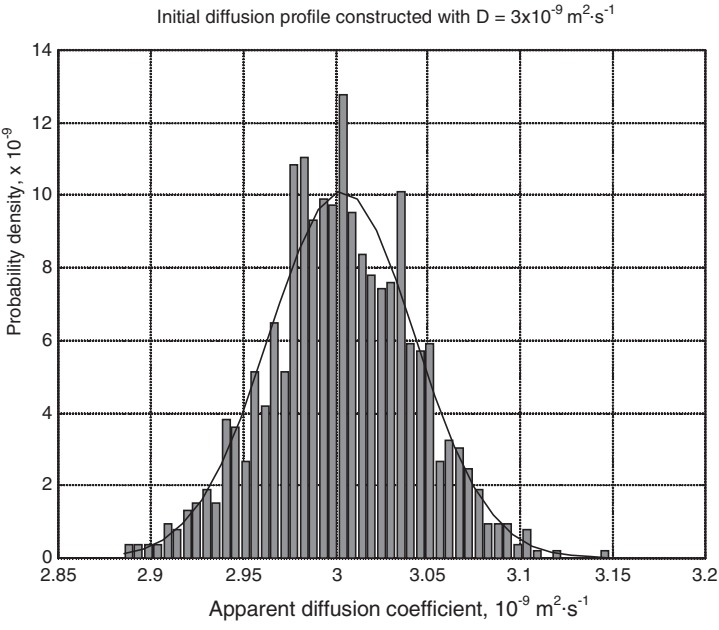

Fig. 6. Typical output of Monte-Carlo simulation showing the probability density of the apparent diffusion coefficient D_{app}. Starting composition profile was built with $D = 3.0 \times 10^{-9}$ m$^2 \cdot$s^{-1}, output of the procedure is $D = 3.0 \pm 0.8 \times 10^{-9}$ m$^2 \cdot$s^{-1}.

uncertainty on the composition measurements: more precisely, we decided to set $\Delta D/D = \pm 2\sigma$, corresponding to a 95% confidence interval. When applied to our data set, the results of the procedure are $\Delta D_{In}/D_{In} = \pm 6\%$, $\Delta D_{Bi}/D_{Bi} = \pm 3\%$, and $\Delta D_{Ni}/D_{Ni} = \pm 3\%$. The higher uncertainty on D_{In} can be ascribed to the fact that the C_0 value for indium is below 1%, i.e., below the threshold where the AAS measurement reaches its full accuracy. It can thus be loosely stated that the indium data points are more prone to error than their bismuth counterparts.

More generally, it appeared interesting to use the Monte Carlo procedure in a parametrical study aimed at the definition of the optimal experimental conditions to improve the accuracy on the diffusion coefficient measurement. The tested variables are as follows: the true diffusion coefficient D itself (values of 3×10^{-9} m$^2 \cdot$s^{-1} and 9×10^{-9} m$^2 \cdot$s^{-1}), the duration t of the diffusion phase (from 10^3 to 4×10^5 s), the initial composition C_0 within the solute-rich half capillary (1, 3, 5, and 10 wt%), the number N and length l of disks ($N = 20$, $l = 3$ mm in the present experiments, $N = 30$, $l = 6$ mm as in Ref. 14). Both absolute and relative uncertainties were considered.

Regarding absolute uncertainties, typical of standard measurement techniques such as AAS or ICP-MS (inductively coupled plasma-mass spectrometry) in the low concentration range, say below 1 wt%, the results show that $\Delta D/D$ is always proportional to $\Delta C_0/C_0$. More generally, the ratio $(\Delta D/D)/(\Delta C_0/C_0)$ can be plotted on a master curve against the quantity $\kappa = (4\pi D_{\text{app}}t)^{1/2}/l$ as shown in Fig. 7. It should be remarked that κ is essentially a measure of the number of points which carry most of the available information on mass transport for the χ^2 minimization procedure, as it represents the spread of the composition profile $(4\pi D_{\text{app}}t)^{1/2}$ normalized by the disk thickness.

As such, the observed $\kappa^{-1/2}$ tendency is not surprising, and can indeed be recovered by simple statistical order-of-magnitude arguments [38]. Another interesting feature of the curve of Fig. 7 is the existence of a minimum at a time corresponding to the spreading of the composition gradient up to the capillary ends. The subsequent decrease of the accuracy on D upon further time increase can be understood as related to the loss of the initial composition information, a useful parameter in the fitting procedure.

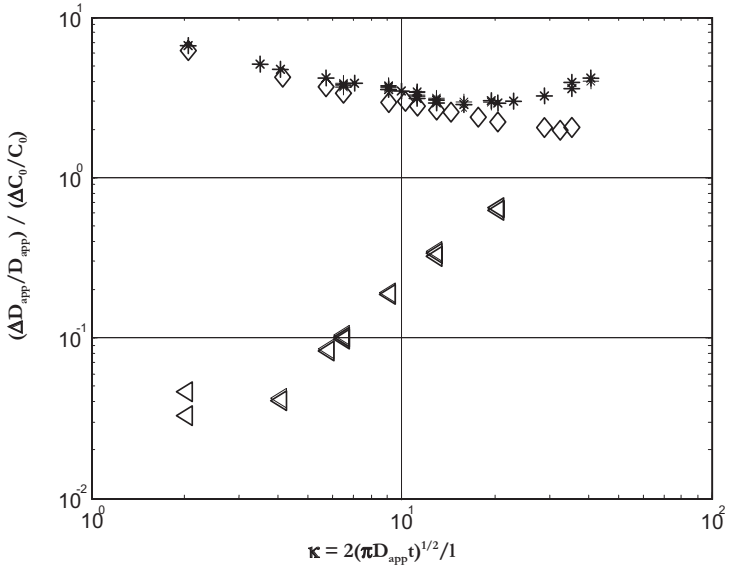

Fig. 7. Normalized relative uncertainty on the diffusion coefficient with absolute [$*$, Foton configuration; $\diamond$, Ref. 14 configuration], and relative type of uncertainty ($\triangleleft$) on the individual composition measurements. The slight difference between the Foton and Ref. 14 configurations is due to the larger number of disks in the latter case.

From a practical standpoint, i.e., with a number of measurement points on the order of 20 to 30, it is seen that the ratio $(\Delta D/D)/(\Delta C_0/C_0)$ for absolute uncertainties is always significantly larger than unity, meaning that the individual composition measurements are a key limitation in improving the accuracy of the diffusivity measurement. As for the variation of $(\Delta D/D)$ with experiment duration, an increase of t_E could be viewed as positive, since the $\kappa^{-1/2}$ behavior corresponds to a $t^{-1/4}$ dependence. However, the limitation in terms of keeping away from the sample ends should not be forgotten. Besides, the $t^{-1/4}$ power law is such that the attainment of a significant accuracy improvement would require unrealistically long capillaries.

Regarding relative uncertainties, striking results were obtained, with predicted accuracies on D remaining very good over a large range of the κ parameter, and in any case much lower than for the associated absolute uncertainties but in the high κ regime where the two curves merge (see Fig. 7). However, such a finding can be qualitatively explained by the structure of the χ^2 criterion; with absolute uncertainties, the contribution of the low composition data points to the sum is negligible, and therefore the information associated with these points is lost in the fit procedure. With relative uncertainties on the other hand, all data points are equally well represented in the χ^2, and all information is available for the fit procedure. The open question is now to identify a composition analysis technique allowing a relative type of uncertainty even in the very low concentration range.

5. DIFFUSIVITY VALUES AND COMPARISONS WITH EXISTING DATA

The primary objective of this section is to specify for each system the diffusivity value, along with a relevant error bar. For the aluminum cell where all four capillaries performed properly, the legitimate choice for an unbiased estimate is to average the four diffusivities and propose $D_{Ni} = 3.7 \times 10^{-9}\ m^2 \cdot s^{-1}$ at $T = 969$ K. We did not attempt a statistical analysis of our four-fold data set, as the small number of measurements available would have rendered the attempt quite meaningless. To account for the observed dispersion, we decided to set $\Delta D_{Ni}/D_{Ni} \approx \pm 10\%$. If we only consider assessed error sources, the estimated overall relative uncertainty should be taken as the sum of the temperature (2%), duration (1.5%), convection (1%), and composition measurement (3%) mechanisms, that is $\Delta D_{Ni}/D_{Ni} \approx \pm 7.5\%$. Both values are relatively close, and it should be recalled that we were not able to quantify the uncertainty coming from the starting capillary homogeneity and possible diffusion barriers coming from the rupture of the oxide film upon the initial shearing.

Regarding the tin cell, the indium diffusion coefficient is $D_{In} = 3 \times 10^{-9}$ $m^2 \cdot s^{-1}$, the estimated overall relative uncertainty being $\Delta D_{In}/D_{In} \approx \pm 9$ % (temperature (2%), duration (0.06%), convection (1%), and composition measurements (6%)) at the working temperature of 574 K. As for bismuth, we can take $D_{Bi} = 2.4 \times 10^{-9}$ $m^2 \cdot s^{-1}$ with an overall relative uncertainty $\Delta D_{Bi}/D_{Bi} \approx \pm 6\%$ (temperature (2%), duration (0.06%), convection (1%), and composition measurements (3%)) again at the working temperature of 574 K. It should again be recalled that we were deprived of the information coming from the experimental data scatter due to a malfunctioning of the volume compensation mechanism in the tin cell. In the absence of this information, along with that coming from the effect of the starting capillary homogeneity, we decided to set in both cases $\Delta D_{In}/D_{In} \approx \pm 10$ % and $\Delta D_{Bi}/D_{Bi} \approx \pm 10$ %. Such a choice may appear rather arbitrary, and one may wonder whether we bothered to carry out all the analysis, but our opinion is that it is better to remain on the safe side.

A second important objective of this section is to make comparisons with our tin system diffusivity data, since a number of published studies deal with both In and Bi impurity diffusion in Sn-based alloys. The first method from a chronological standpoint relies on the analysis of a quenched solidification front, as carried out by Verhoeven et al. [7]. Advantage was taken from the fact that, for purely diffusion-controlled solute transport conditions, a growth front advancing at a velocity V_I is preceded by a solute-rich boundary layer where the composition profile decreases exponentially over a length scale D/V_I from its interface value C_∞/k to its far field value C_∞, k being the segregation coefficient of the solute. It is thus possible, from a fit of the composition profile, to extract a value for the diffusion coefficient. This was done by Verhoeven et al. for tin-based alloys with nominal compositions up to 3.5 at% Bi. In dilute systems, assuming a value $k = 0.29$, their results can be summarized as $D_{Bi} = 1.8 \times 10^{-9}$ $m^2 \cdot s^{-1}$, with an uncertainty that should be taken as $\pm 10\%$.

The diffusivity result is given at the melting temperature of tin, but a difficulty in assessing the validity of the results is that the diffusion takes place in a strong vertical thermal gradient to stabilize the interface against morphological instability. This results in temperature variations over the enriched solutal boundary layer thickness D/V_I in excess of 20 K. Another difficulty is that the thermal gradient, if not perfectly directed axially along the sample can in turn induce some natural convection, which in turn may prevent the full development of the solutal boundary layer ahead of the growth front. It should be acknowledged that those factors, along with possible thermodiffusion solute fluxes, are discussed by Verhoeven et al. [7] in their thorough characterization of their experimental conditions, but an adverse impact can never be excluded.

The quenched solidification front technique was also used on the occasion of the Mephisto microgravity USMP1 [25] and USMP3 [39] experiments, which featured Sn:0.58 at% Bi alloys. The composition profiles analysis was carried out with a value $k = 0.27$ originating from the measurement of the solidification interval. It should be noted that phase diagram data [40, 41] indicate a value closer to $k = 0.29$, but a 10% relative error on k can not be excluded adding in the uncertainties in terms of liquidus and solidus slopes. The results obtained are slightly different between the USMP1 and USMP3 experiments, namely $D_{Bi} = 1.3 \times 10^{-9}$ $m^2 \cdot s^{-1}$ and $D_{Bi} = 1.5.10^{-9}$ $m^2 \cdot s^{-1}$, but significantly lower than the estimate by Verhoeven et al. [7], $D_{Bi} = 1.8 \times 10^{-9}$ $m^2 \cdot s^{-1}$.

To account for the discrepancy, we attempted to check the sensitivity of the D_{Bi} best-fit results on the value of other process and thermophysical parameters, namely V_I, C_∞, and k. For instance, relative variations of the instantaneous solidification rate between ± 5 % are not to be excluded, even though hardly measurable directly. Such variations will induce a similar $\pm 5\%$ uncertainty in terms of D. Regarding the partition coefficient, we found that a shift in k from 0.27 to 0.32 led to an increase from $D_{Bi} = 1.3 \times 10^{-9}$ $m^2 \cdot s^{-1}$ to $D_{Bi} = 1.7 \times 10^{-9}$ $m^2 \cdot s^{-1}$. Even more important is that a change of C_∞ from 0.58 at% to 0.56 at%, e.g., due to radial segregation, was found to amount to a 10% relative variation in terms of D_{Bi}.

In summary, and considering the uncertainty on k and the fact that V_I and C_∞ are not fully controllable parameters, the results obtained by the quenched solidification technique should be considered with caution. Nevertheless, it should be remarked that the data of Verhoeven et al. [7], when extrapolated to our working temperature using Eq. (4) with $n = 2$, yield $D_{Bi} = 2.35 \times 10^{-9}$ $m^2 \cdot s^{-1}$ in very good agreement with the Foton data.

Long capillary experiments, similar in principle to shear cell arrangements except for their beginning (the half capillaries are in contact in the solid state and rapidly heated) and their ending (the composition profile is quenched), were implemented by Frohberg and coworkers [42] on a variety of metallic systems in microgravity experiments. Regarding impurity diffusion of In in Sn, the extrapolated value at our working temperature using again Eq. (4) with $n = 2$ is $D_{In} = 3.6 \times 10^{-9}$ $m^2 \cdot s^{-1}$. Such a value is relatively close, though significantly larger, than what has been measured in the present work, but our opinion is that shear cell techniques allow better control of the experiment and thus result in more accurate measurements.

On a related line of work, the results recently obtained by Botton et al. [14, 38], using a shear cell technique similar in principle to that used in the AGAT experiment, are worth mentioning; their key idea is to use a constant magnetic field to control, rather than fully suppress, natural convection. When buoyancy is mostly due to the interaction of the temperature

gradients with gravity, theoretical arguments show that the additional transport results in a modified error function profile featuring an apparent diffusion coefficient which accounts for the presence of convection.

The experimental procedure is then to apply a carefully controlled temperature gradient of the order of $100\ \mathrm{K \cdot m^{-1}}$ and to carry out measurements at various values of the magnetic field to obtain an estimate of D. This was done for In impurity diffusion in Sn-based alloys, a striking feature of this system being that tin and indium have very similar densities. The result obtained is $D_{\mathrm{In}} = 2.55 \times 10^{-9}\ \mathrm{m^2 \cdot s^{-1}}$ at a mean temperature $T = 548$ K with a $\pm 5\%$ error bar.

The situation is much more complex for the case of Bi impurity diffusion, since convection due to solutal buoyancy, unsteady in nature, requires a more intricate theoretical treatment [13, 14, 43]. Suffice it to say here that the measured value is $D_{\mathrm{Bi}} = 2.05 \times 10^{-9}\ \mathrm{m^2 \cdot s^{-1}}$, again at a mean temperature $T = 548$ K and a $\pm 8\%$ error bar. When transformed to our Foton working temperature of 574 K using Eq. (4) with $n = 2$ for purposes of comparison, we obtain $D_{\mathrm{In}} = 2.80 \times 10^{-9}\ \mathrm{m^2 \cdot s^{-1}}$ and $D_{\mathrm{Bi}} = 2.25 \times 10^{-9}\ \mathrm{m^2 \cdot s^{-1}}$.

As such, the good agreement observed between values obtained in two different setups in different conditions (microgravity versus magnetic fields) are a clear indication of the validity of the results. From the analysis of the literature database, a set of coherent diffusivity values for bismuth as a function of temperature is reported in Table I.

Our opinion is that direct measurements where only Fick's law is involved are the best way to estimate physically sound diffusivity data, and that shear cell devices are probably optimal for experimental implementation. On the other hand, techniques based on the analysis of quenched solidification profiles are prone to a variety of errors, due to the difficulty of mastering the growth process and assessing the value of other thermophysical parameters. The same can be said of all indirect techniques, especially those featuring a poorly controlled fluid flow.

Table I. Summary of Recommended Values for the Bismuth Diffusion Coefficient in Tin

Temperature (K)	Diffusivity ($10^{-9}\ \mathrm{m^2 \cdot s^{-1}}$)	Reference
574	2.4 ±10%	Present work
548	2.05± 8%	43
504	1.8 ±10%	7

6. CONCLUDING REMARKS

Our objective in this paper was to present in some detail the results of the microgravity solute diffusion coefficient measurements carried out on tin- and aluminum- based alloys during the Foton 12 mission. Regarding the tin cell, the data for In and Bi can be summarized as $D_{\mathrm{In}} = 3 \times 10^{-9}$ $\mathrm{m}^2 \cdot \mathrm{s}^{-1}$, and $D_{\mathrm{Bi}} = 2.4 \times 10^{-9}$ $\mathrm{m}^2 \cdot \mathrm{s}^{-1}$ at $T = 574$ K. As for the aluminum cell, we obtained for the Ni diffusivity $D_{\mathrm{Ni}} = 3.7 \times 10^{-9}$ $\mathrm{m}^2 \cdot \mathrm{s}^{-1}$ at $T = 969$ K. In all cases, the ascribed relative uncertainty were taken to be $\pm 10\%$. Such a $\pm 10\%$ value may appear deceptively high, especially since we were not able to quantify all error sources, but it comes at least from what we think is a thorough analysis of the possible perturbation mechanisms. As such, our data can hardly be used for the assessment of the validity of atomic-scale transport mechanisms, but it can find fruitful applications in the field of process (e.g., solidification) modeling. Comparison with existing data, when available, showed that our measurements are in good agreement with values proposed in the frame of a program aimed at control of the natural convection by means of magnetic fields.

Apart from a few minor improvements related to the implementation of the shear cell experiment, the key to a significant reduction in the error bars appears to be the identification of a composition measurement technique allowing a relative type of uncertainty in the very low concentration range. Indeed, a limiting factor is that a χ^2 minimization procedure based on data from standard analysis methods, such as AAS or ICP-MS, can not account for the information contained in the lower range of the concentration profile. On the other hand, one of the important results of the Monte-Carlo simulations carried out in this paper is to show that relative errors on the composition measurements may result in a much lower uncertainty for the diffusion coefficient, provided a suitable measurement technique can be identified.

ACKNOWLEDGMENTS

It is a pleasure to thank our colleagues P. Dusserre, J. P. Praizey, C. Salvi, and J. Abadie from CEA-Grenoble, as well as G. Frohberg and K. H. Kraatz from TU Berlin for their help during the experiment preparation. For CEA staff, the present work was carried out within the frame of the now defunct GRAMME agreement between the CNES and the CEA.

REFERENCES

1. Z. Guo, S. Maruyama, and A. Komiya, *J. Phys. D* **32**:995 (1999).
2. L. B. Jalbert, R. M. Banish, and F. Rosenberger, *Phys. Rev. E* **57**:1727 (1998).

3. F. Debray, Y. Fautrelle, and F. Dalard, *Exp. Fluids* **19**:353 (1995).
4. N. Simon, T. Flament, A. Terlain, and C. Deslouis, *Int. J. Heat Mass Transfer* **38**:3085 (1995).
5. C. Allibert, P. Marty, A. Gagnoud, and Y. Fautrelle, *Int. J. Heat Mass Transfer* **43**:437 (2000).
6. P. S. Dutta and A. G. Ostrogorsky, *J. Crystal Growth* **217**:360 (2000).
7. J. D. Verhoeven, E. D. Gibson, and R. I. Griffith, *Met. Trans. B* **6**:475 (1975).
8. T. Ujihara, K. Fujiwara, G. Sazaki, N. Usami, and K. Nakajima, *J. Crystal Growth* **241**:387 (2002).
9. A. Griesche, K. H. Kraatz, and G. Frohberg, *Rev. Sci. Instrum.* **69**:315 (1998).
10. G. Müller-Vogt and R. Kössler, *J. Crystal Growth* **186**:511 (1998).
11. P. Bräuer and G. Müller-Vogt, *J. Crystal Growth* **186**:520 (1998).
12. J. P. Garandet, J. P. Paizey, S. Van Vaerenbergh, and T. Alboussière, *Phys. Fluids* **9**:510 (1997).
13. D. McLean and T. Alboussière, *Int. J. Heat Mass Transfer* **44**:1639 (2001).
14. V. Botton, P. Lehmann, R. Bolcato, R. Moreau, and R. Haettel, *Int. J. Heat Mass Transfer* **44**:3345 (2001).
15. G. Taylor, *Proc. Roy. Soc. London Ser. A* **219**:186 (1953).
16. G. Mathiak and G. Frohberg, *Cryst. Res. Technol.* **34**:181 (1999).
17. G. Mathiak, A. Griesche, K. H. Kraatz, and G. Frohberg, *J. Non-Crystalline Solids* **205**:412 (1996).
18. R. W. Smith, *Microgravity Sci. Technol.* **XI/2**:78 (1998).
19. J. I. D. Alexander and R. M. Banish, *Microgravity Sci. Technol.* **XI**:90 (1998).
20. R. Savino and R. Monti, *Int. J. Heat Mass Transfer* **42**:111 (1999).
21. S. Matsumo and S. Yoda, *J. Appl. Phys.* **85**:8131 (1999).
22. R. J. Naumann, *Int. J. Heat Mass Transfer* **43**:2917 (2000).
23. G. Mathiak and R. Willnecker, in *First Int. Symp. on Microgravity Research and Applications in Physical Sciences and Biotechnology*, Sorrento, Italy, Vol. ESA SP-454, p. 513 (2000).
24. V. Botton, J. P. Garandet, T. Alboussière, and P. Lehmann, *J. Physique IV France* **11-PR6**:57 (2001).
25. J. J. Favier, P. Lehmann, J. P. Garandet, B. Drevet, and F. Herbillon, *Acta Mater.* **44**:4899 (1996).
26. M. D. Dupouy, D. Camel, and J. Abadie, *Materials Science Forum* **329/330**:305 (2000).
27. A. Griesche, K. H. Kraatz, G. Frohberg, G. Mathiak, and R. Willnecker, in *First Int. Symp. on Microgravity Research and Applications in Physical Sciences and Biotechnology*, Sorrento, Italy, Vol. ESA SP-454, p. 497 (2000).
28. W. A. Arnold and D. Matthiesen, *J. Electrochem. Soc.* **142**:433 (1995).
29. Z. Zeng, H. Mizuseki, K. Ichinoseki, and Y. Kawazoe, *Num. Heat Transfer*, Part A **34**:709 (1998).
30. J. P. Garandet, P. Dusserre, J. P. Praizey, J. Abadie, A. Griesche, and V. Botton, *J. Microgravity Space Station Utilization* **1**:29 (2000).
31. J. Crank, in *The Mathematics of Diffusion* (Clarendon Press, Oxford, 1956).
32. H. Hamacher, H. E. Richter, S. Drees, A. V. Egorov, A. S. Senchenkov, M. V. Volkov, and P. Sickinger, in *50th Int. Astronautical Congress*, Amsterdam, The Netherlands, Vol. IAF-99-J, p. 3.05 (1999).
33. A. Griesche, S. Suzuki, K. H. Kraatz, G. Frohberg, G. Mathiak, and R. Willnecker, to be published.
34. G. Frohberg, K. H. Kraatz, and H. Wever, in *Proc. Conf. "Scientific Results of the German Spacelab Mission D1," Norderney 1986*, P. R. Sahm, R. Jansen, and M. H. Keller, eds. (Wissenschaftliche Projektführung D1, c/o DLR Cologne, 1987), pp. 144–147.

35. A. Griesche, Ph.D. thesis (TU Berlin, 1995) [in German].
36. P. Bräuer, Ph.D. thesis (Univ. Karlsruhe, 1995) [in German].
37. R. Kössler, Ph.D. thesis (Univ. Karlsruhe, 1990) [in German].
38. V. Botton, Ph.D. thesis (INP-Grenoble, 2001) [in French].
39. G. Boutet, Ph.D. thesis (Paris VI, 1999) [in French].
40. T. B. Massalski, H. Okamoto, P. R. Subramanian, and L. Kacprzak, eds., in *Binary Alloys Phase Diagrams*, Vol. 1 (ASM International, Materials Park, Ohio, 1990).
41. B. J. Lee, C. S. Oh, and J. H. Shim, *J. Electron. Mater.* **25**:983 (1996).
42. G. Frohberg, K. H. Kraatz, A. Griesche, and H. Wever, Diffusion in liquid metal alloys: Self- and impurity diffusion, in *Symp. on Scientific Results of the German Spacelab Mission D2, Norderney, ISBN 3-89100-025-1 (1994)*, pp. 288–294
43. V. Botton, P. Lehmann, R. Bolcato, and R. Moreau, *Int. J. Heat Mass Transfer* **47**:2457 (2004).